PREDICTION OF MAXIMUM SCOUR DEPTH AROUND SPUR-DIKE-LIKE STRUCTURES

Md. Munsur RAHMAN[1] and Yoshio MURAMOTO[2]

[1]Student Member of JSCE, Graduate Student, Dept. of Civil Engineering, Kyoto University (Yoshida Honmachi, Sakyo-Ku, Kyoto 606-8317, Japan)

[2]Fellow of JSCE, Dr. of Eng., Professor, Dept. of Civil Engineering, Kyoto University (ditto)

Some features of flow and scouring around spur-dike-like structures (or abutments) are discussed based on experiments under clear-water scouring. A simplified analytical model for the prediction of the maximum scour depth around these kinds of structures is developed by considering flow concentration to a restricted region in the scour hole. The model predicts scour depth at sloped-wall as well as at vertical-wall abutments, being verified by the available data and previous formulae. Finally, a model constant for flow concentration is identified by the inversion of experimental data, and an interpolated analytical model for the maximum scour depth under low and high tractive forces.

Key Words: *abutment, clear-water scour, maximum scour depth, analytical model*

1. INTRODUCTION

Spur-dike-like structures are the structures extended from the bank towards the transverse direction of a river. As these kinds of structures, there are spur-dikes, groynes, bridge abutments, guide bunds, river closer works, etc. The natural flow is disturbed and intensified locally by the existence of these kinds of structures, and consequently the local scouring occurs until the equilibrium condition attains. In the present study, spur-dike-like structures are called hereafter as abutments for the simplicity of naming.

The maximum scour depth is one of the important factors for the safe and economic design of abutments. The previous prediction methods so far available can be classified into three groups, namely, empirical formulae[1),2),3)], analytical models[4),5),6)], and numerical models[7),8)]. Numerical models are most useful for the detailed engineering design, however, being still in developing stages, and take long computational time for each type of river structures and hydraulic conditions.

On the other hand, previous experiments on flow properties around abutments are rather limited as compared to those around bridge piers. However, from flow measurements in the scoured bed at abutments, the strongest concentration of flow near the abutment edge and at the base of the scour hole was found[2),9)].

The present study is limited to the clear-water scouring around a single and non-submerged abutment, and aimed at the following objectives. First, to discuss some experimental features of flow and scouring around vertical and sloped-wall abutments. Second, to develop a simplified model to predict the maximum scour depth around abutments. Third, to test the developed model against the available data and other previous formulae, and then to elucidate the dominant parameter for the maximum scour depth. Finally, some critical points about the model constant β for flow concentration are discussed.

2. EXPERIMENTS

(1) Methodology

Experiments were conducted in a 10m long, 1m wide and 0.2m deep flume. A typical shape of the sloped-wall abutments used and the experimental conditions together with some results are shown in **Fig. 1** and **Table 1**, respectively. The hydraulic quantities in **Table 1** are the flow conditions in the far upstream of the abutment location.

During the experiments, the outline and depth of scour hole were recorded manually, and in the final state, the detailed bed-level data were obtained by using a laser sensor connected with a personal computer. In Run V-1 and S-3, flow velocities were measured at both flat and scoured bed using a 2-D electro-magnetic velocity meter.

Table 1 Experimental conditions.

Model	Run	b (cm)	i	Q (l/s)	h (cm)	u (cm/s)	u_* (cm/s)	b/B	b/h	Fr	τ_*/τ_{*c}	d_s (cm)	d_s/h	ϕ (Deg.)	t (min)
V1H0[u]	V-1	10.0	1/500	4.24	2.15	24.7	2.05	0.13	4.7	0.54	0.49	3.20	1.49	26.6	2880
V1H0	V-2	12.5	1/500	4.24	2.15	24.7	2.05	0.16	5.8	0.54	0.49	4.20	1.95	28.1	3055
V1H0	V-3	15.0	1/500	4.24	2.15	24.7	2.05	0.19	7.0	0.54	0.49	5.40	2.51	28.0	4080
V1H0	V-4	20.0	1/500	4.24	2.15	24.7	2.05	0.25	9.3	0.54	0.49	6.60	3.07	35.0	2730
V1H0	V-5	10.0	1/200	3.40	1.43	29.7	2.65	0.13	7.0	0.79	0.82	4.60	3.22	26.6	155
V1H0	V-6	15.0	1/200	3.40	1.43	29.7	2.65	0.19	10.5	0.79	0.82	6.00	4.20	24.8	150
V1H0	V-7	20.0	1/200	3.40	1.43	29.7	2.65	0.25	14.0	0.79	0.82	7.20	5.03	23.9	175
V1H0	V-8	10.0	1/200	4.24	1.63	32.5	2.83	0.13	6.1	0.81	0.93	5.80	3.56	26.6	240
V1H0	V-9	12.5	1/200	4.24	1.63	32.5	2.83	0.16	7.7	0.81	0.93	6.80	4.17	25.8	220
V1H0	V-10	15.0	1/200	4.24	1.63	32.5	2.83	0.19	9.2	0.81	0.93	7.60	4.66	28.6	120
V1H0.5	S-1	12.0	1/500	4.24	2.15	24.7	2.05	0.15	5.6	0.54	0.49	3.87	1.80	31.0	2880
V1H1	S-2	13.9	1/500	4.24	2.15	24.7	2.05	0.17	6.5	0.54	0.49	2.77	1.29	29.3	2585
V1H2[u]	S-3	17.9	1/500	4.24	2.15	24.7	2.05	0.22	8.3	0.54	0.49	3.76	1.75	31.0	4320
V1H3	S-4	21.8	1/500	4.24	2.15	24.7	2.05	0.27	10.1	0.54	0.49	4.02	1.87	32.6	4400
V1H1	S-5	14.2	1/200	4.24	1.63	32.5	2.83	0.18	8.7	0.81	0.93	4.16	2.55	26.6	140
V1H2	S-6	18.4	1/200	4.24	1.63	32.5	2.83	0.23	11.3	0.81	0.93	4.25	2.61	31.0	240
V1H3	S-7	22.6	1/200	4.24	1.63	32.5	2.83	0.28	13.8	0.81	0.93	4.45	2.73	26.6	240

B=80cm, d=0.142cm (uniform sand: $\sqrt{d_{86}/d_{14}}$ = 1.28), V1H0: vertical-wall abutments, V1H0.5 ~V1H3 (V/H = tanθ): sloped-wall abutments, V1H0[u] and V1H2[u]: velocity measurements at initial and final states.

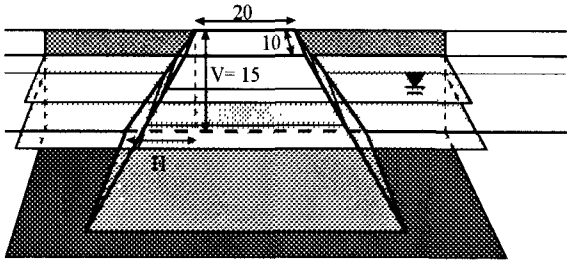

Fig. 1 Dimensions of sloped-wall abutments (unit: cm).

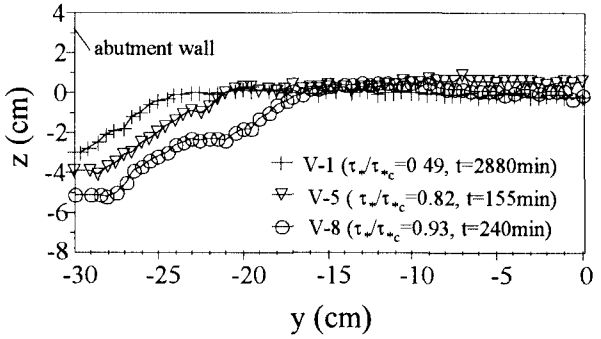

Fig. 2 (a) Lateral bed profiles of scour hole around vertical-wall abutments at the final stage.

(2) Depending parameters

The functional relationship of the maximum scour depth (d_s) with other factors in the present experiments can be expressed as

$$d_s = f(B, h, b, i, d, \theta) \qquad (1)$$

where d_s = maximum scour depth, B = channel width, h = flow depth, b = lateral length of the abutment, i = bed slope, d = sediment diameter, and

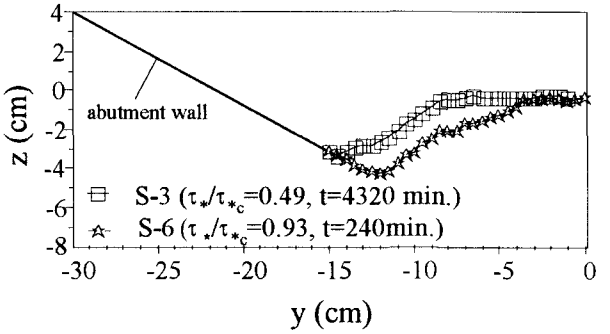

Fig. 2 (b) Lateral bed profiles of scour hole around sloped-wall abutments at the final stage.

θ = side slope of abutment. In the present study, we used the following dimensionless parameters, and listed in **Table** 1.

$$d_s/h = f(b/B, b/h, Fr, \tau_*/\tau_{*c}, \theta) \qquad (2)$$

where Fr = Froude number, τ_* = dimensionless tractive force (shear stresses), τ_{*c} = dimensionless critical tractive force for sediment movement.

(3) Experimental results

(a) Lateral bed profiles of the scour holes

Typical lateral bed profiles of scour hole at the final stage are shown in **Fig. 2** (**a**) and (**b**) for the vertical-wall abutments (Run V-1, 5 and 8) and sloped-wall abutments (Run S-3 and 6), respectively. For low values of τ_*/τ_{*c}, the cross-sectional shape of scour hole is triangular, whereas, trapezoidal shapes of scour hole are found near the threshold condition for sediment movement in approach flows.

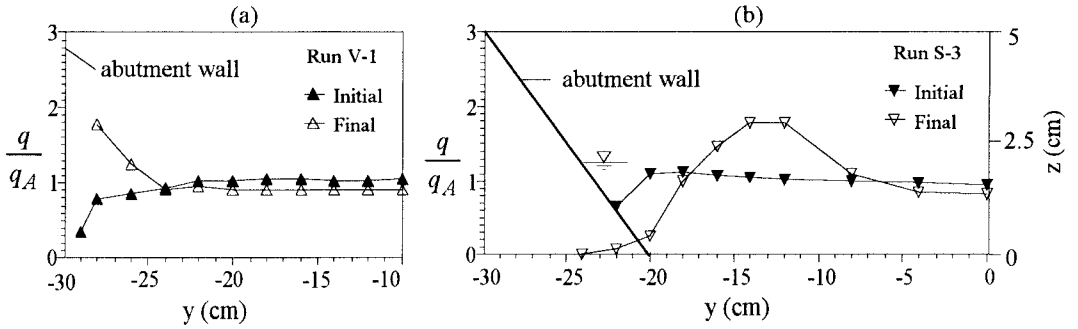

Fig. 3 Lateral distributions of unit discharge at the vertical-wall abutment and sloped-wall abutment (q: unit discharge at an arbitrary position, q_A: the mean unit discharge of approach flow).

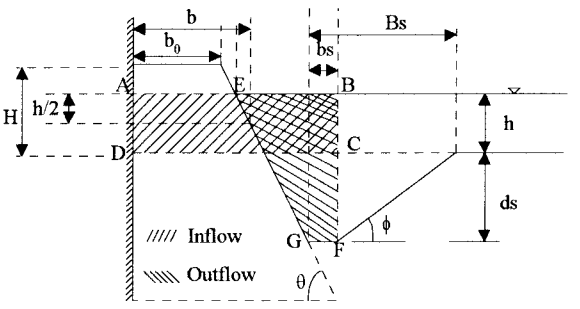

Fig. 4 Definition sketch of the restricted flow concentration model at a sloped-wall abutment.

(b) Lateral distributions of unit discharge

Distributions of unit discharge at the initial and final stages along the lateral direction of the vertical-wall (Run V-1) and sloped-wall abutments (Run S-3) are shown in **Fig. 3 (a)** and **(b)**, respectively. In the final stage, the unit discharge increases in the scour hole region as compared with that in the flat bed condition. The more manifest features of flow concentration can be found in the previous experimental studies[2),9)].

3. MODEL DEVELOPMENT

Considering the above experimental features, we developed a simplified model for the maximum scour depth prediction using the continuity relation between the inflow and outflow in the restricted flow concentration region of a scour hole. The schematic cross-sectional view of a scour hole at the sloped-wall abutment is shown in **Fig. 4**.

Inflow (ABCD area) =

$$\left(b + h/2\tan\theta + b_s + d_s/\tan\theta\right)uh \tag{3}$$

Outflow (EBFG area) =

$$\left\{h^2/2\tan\theta + \left(b_s + d_s/\tan\theta\right)h + \left(b_s + d_s/2\tan\theta\right)d_s\right\}u_s \tag{4}$$

$$b_s = \beta B_s = \left\{\beta/(1-\beta)\right\}\left(d_s/\tan\phi\right) \tag{5}$$

where $b = b_0 + (2H - h)/2\tan\theta$, u = mean velocity of approach flow, u_s = mean velocity in the EBFG region, ϕ = rest angle, and β = constant (<1) for flow concentration.

From Eqs. (3)~(5), we obtain the following quadratic equation on $\tilde{d}_s$ in the equilibrium state of clear-water scouring ($u_s = u_c$, u_c: critical velocity for sediment movement).

$$\tilde{d}_s^{\,2} + a_1(1-\tilde{u})\tilde{d}_s - a_2\left\{\tilde{u}\left(\tilde{b} + 1/2\tan\theta\right) - 1/2\tan\theta\right\} = 0 \tag{6}$$

where $\tilde{d}_s = d_s/h$, $\tilde{u} = u/u_c$, $\tilde{b} = b/h$, $a_1 = 1 + \left\{1 + (2\beta\tan\theta)/(1-\beta)\tan\phi\right\}^{-1}$ and $a_2 = \left\{\beta/(1-\beta)\tan\phi + 1/2\tan\theta\right\}^{-1}$.

Solving Eq. (6) for $\tilde{d}_s$

$$\tilde{d}_s = 0.5\left[-a_1(1-\tilde{u}) + \sqrt{\left\{a_1(1-\tilde{u})\right\}^2 + 4a_2\left\{\tilde{u}\left(\tilde{b} + 1/2\tan\theta\right) - 1/2\tan\theta\right\}}\right] \tag{7}$$

When we assume the velocity coefficient u/u_* is constant and put $\tilde{u} = u_*/u_{*c} = \left(\tau_*/\tau_{*c}\right)^{0.5} = \tilde{\tau}_*^{\,0.5}$ in Eq. (7), $\tilde{d}_s$ for the vertical abutment (θ = 90°) is expressed as

$$\tilde{d}_s = 0.5\left\{-\left(1 - \tilde{\tau}_*^{\,0.5}\right) + \sqrt{\left(1 - \tilde{\tau}_*^{\,0.5}\right)^2 + 4\tan\phi\,\tilde{\tau}_*^{\,0.5}\,\tilde{b}(1-\beta)/\beta}\right\} \tag{8}$$

When the approach flow is under the threshold condition ($\tilde{u} = 1$ or $\tilde{\tau}_* = 1$) for sediment movement, Eqs. (7) and (8) are simply expressed as Eqs. (9) and (10), respectively.

For sloped-wall abutments

$$\tilde{d}_s = \sqrt{a_3\tilde{b}} \tag{9}$$

where $a_3 = \left\{\beta/\tan\phi(1-\beta) + 1/2\tan\theta\right\}^{-1}$

For vertical-wall abutments

$$\tilde{d}_s = \sqrt{\left\{\tan\phi(1-\beta)/\beta\right\}\tilde{b}} \tag{10}$$

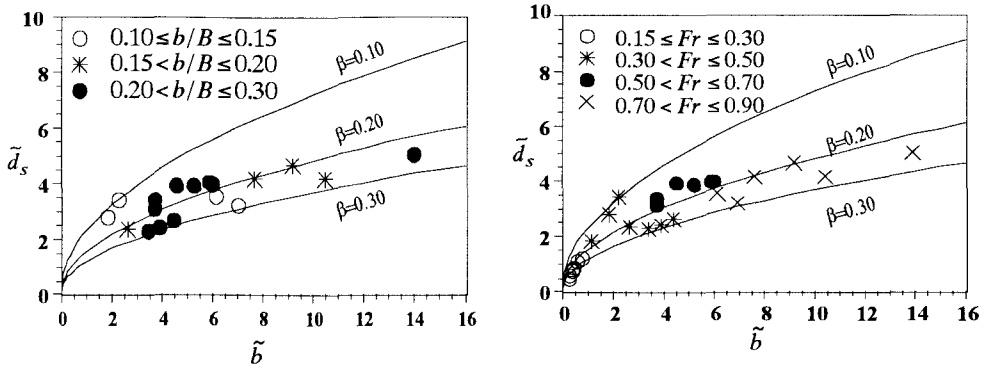

Fig. 5 Relation between $\tilde{d}_s$ and $\tilde{b}$ (parameters: b/B, Fr) for $0.80 \le \tilde{\tau}_* \le 1.0$.

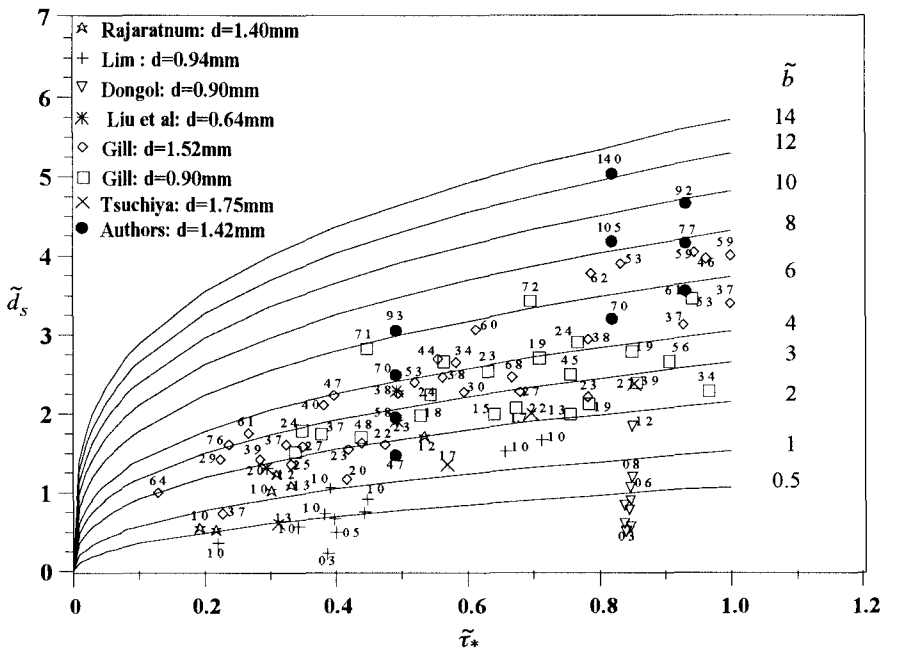

Fig. 6 Relation between $\tilde{d}_s$ and $\tilde{\tau}_*$ for given values of $\tilde{b}$ under the clear-water scouring condition (added figures of plotted data $=\tilde{b}$).

4. MODEL VERIFICATION

(1) Maximum scour depth for vertical-wall abutments

(a) Determination of the β-value and effect of hydraulic parameters on the scour depth

The effects of dimensionless hydraulic parameters, b/B and Fr, on the maximum scour depth are examined in the $\tilde{d}_s - \tilde{b}$ plane as shown in **Fig. 5**. The plotted data, which include the previous experimental results[2),3),6)] together with the present ones, are at vertical abutments near the threshold condition for sediment movement ($0.8 \le \tilde{\tau}_* \le 1.0$). The solid lines are calculated from Eq. (10) for different values of β and tanϕ = 0.58 (ϕ = 30°) which is corresponding to the average value of the present experiment (**Table 1**). As far as the available data ($0.10 \le b/B \le 0.30$ and $0.15 \le Fr \le 0.9$), it can be seen that $\tilde{d}_s$ has no clear dependence on b/B and Fr under a constant value of $\tilde{b}$. The calculated curve for $\beta = 0.20$ fits in average with the existing data. β is a very important constant in the present model, and may not be constant for the wide ranges of $\tilde{b}$ or $\tilde{\tau}_*$. These facts will be discussed later. But to ease the present discussion, β is assumed as a constant (=0.20) hereafter.

In **Fig. 6**, the calculated curves by using Eq. (8) are compared with the observed data[2),3),6)]. For the larger values of $\tilde{\tau}_*$, the calculated curves become closer to the observed data. However, the observed data of $\tilde{d}_s$ are widely scattered for constant values of $\tilde{\tau}_*$ and $\tilde{b}$, especially for the lower values of $\tilde{\tau}_*$. One of the reasons will be the inaccuracy of the data at the estimated equilibrium state of the maximum scour depth because it takes very long time to reach the equilibrium for clear-water scouring[6)].

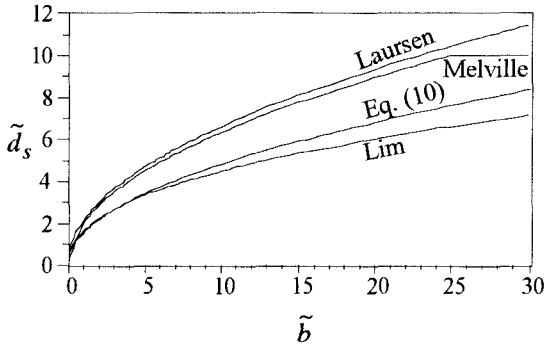

Fig. 7 Comparison of the present model of Eq. (10) with the previous formulae for the maximum scour depth around vertical-wall abutments.

Table 2 Comparison of shape factors obtained from the present model with those proposed by Melville.

Parameters	V1 H0.5	V1 H1	V1 H1.5
tanθ	2.00	1.00	0.67
K_{SM}	0.60	0.50	0.45
K_{SC}	0.80	0.68	0.60
K_{SM}/K_{SC}	0.75	0.74	0.75

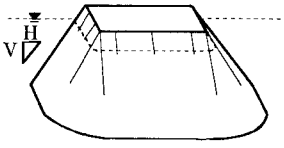

Fig. 8 Spill-through abutment.

(b) Comparison with the previous formulae

In **Fig. 7**, the present model (Eq.(10)) is compared with previously proposed formulae by Laursen[4], Melville[3] and Lim[6] for the prediction of the maximum scour depth ($\tau_* = \tau_{*c}$). The prediction by the present model is situated in the middle of the previous formulae.

(2) Maximum scour depth for sloped-wall abutments

(a) Comparison with Melville's shape factors

Designating $\tilde{d}_s$ in Eq. (8) for vertical-wall abutments as $\tilde{d}_{sv}$ and $\tilde{d}_s$ in Eq. (7) for sloped-wall abutments as $\tilde{d}_{ss}$, the shape factor (K_S) for the threshold condition ($\tilde{u} = 1$) can be defined as

$$K_{sc} = \frac{\tilde{d}_{ss}}{\tilde{d}_{sv}} = \left(1 + \frac{(1-\beta)\tan\phi}{2\beta\tan\theta}\right)^{-1/2} \qquad (11)$$

On the other hand, Melville[3] proposed K_S which depends on θ only for the spill-through type abutment (**Fig. 8**). K_{SC} of Eq. (11) is independent on $\tilde{b}$ and qualitatively corresponds to Melville's K_S. Putting Melville's K_S as K_{SM}, the comparison of K_{SM} and K_{SC} calculated from Eq. (11) (β = 0.20, tanϕ =0.58) for different values of θ is shown in **Table 2**.

It should be noticed that K_{SM}/K_{SC} takes the nearly constant values of 0.75. This is because spill-through type abutments have smooth edge.

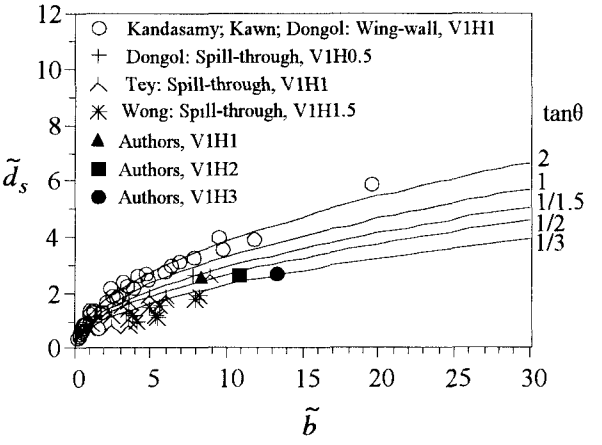

Fig. 9 Comparison of Eq. (9) with the observed data of the maximum scour depth around sloped-wall abutments.

(b) Comparison with the experimental data

The maximum scour depth around sloped-wall abutments calculated by Eq. (9) is compared with the available data in **Fig. 9**. The calculated curves have the similar tendency with the data. There is good agreement with the data of present experimental results.

5. IDENTIFICATION OF THE MODEL CONSTANT β

At the lower value of $\tilde{\tau}_*$, the scour hole around abutments takes a triangular geometry (**Fig. 2**). Under these conditions, the flows concentrate the whole area of scour hole even at the final stage. Therefore, a whole flow concentration model with a triangular cross-section needs to be developed instead of the restricted flow concentration model.

Equating the water balance of inflow (area: ABCD) and outflow (area: EBCF) shown in **Fig. 10**, $\tilde{d}_s$ in the case of vertical-wall abutments (θ = 90°) can be derived as

$$\tilde{d}_s = -(1-\tilde{u}) + \sqrt{(1-\tilde{u})^2 + 2\tan\phi\,\tilde{b}\,\tilde{u}} \qquad (12)$$

Now, we consider a functional relation of Eq. (8) which converges to Eq. (12) as $\tilde{u} \to 0$, and to Eq. (8) taking β = 0.2 for $\tilde{u} \to 1$. Putting $\tilde{d}_s$ of Eqs. (12) and (8) as $\tilde{d}_{s1}$ and $\tilde{d}_{s2}$, respectively, and then we assume a simple interpolated function of $\tilde{d}_{s2}$ as

$$\tilde{d}_{s2} = (1-\tilde{u})\tilde{d}_{s1} + \tilde{u}\tilde{d}_{s2}\big|_{\beta=0.2} \qquad (13)$$

Solving Eq. (13) for β, we obtain the following expression.

$$\beta = \left[1 + f(\tilde{u})/4c_2\right]^{-1} \qquad (14)$$

where $c_2 = \tilde{b}\tan\phi$, and

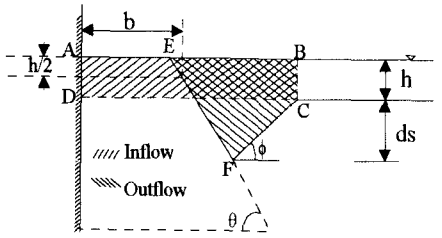

Fig. 10 Definition sketch of the whole flow concentration model with triangular cross section of scour hole around a sloped abutment.

$$f(\tilde{u}) = 2(1-\tilde{u})^3(2-3\tilde{u}) + 8c_2\tilde{u}(3\tilde{u}^3 - 2\tilde{u} + 1) - 4(1-\tilde{u})^3\sqrt{(1-\tilde{u})^2 + 2c_2\tilde{u}} - 2\tilde{u}(1-\tilde{u})^2\sqrt{(1-\tilde{u})^2 + 16c_2\tilde{u}} + 4\tilde{u}(1-\tilde{u}) \times \sqrt{(1-\tilde{u})^4 + 18c_2u(1-\tilde{u})^2 + 32c_2{}^2\tilde{u}^2}$$

On the other hand, the inversion values of β can be obtained from Eqs. (3)~(5) at the equilibrium condition ($u_s = u_c$) for vertical abutments (θ =90°) as below.

$$\beta = \left\{1 + \frac{\tilde{d}_s{}^2 + \tilde{d}_s\left(1-\tilde{\tau}_*{}^{0.5}\right)}{0.58\,\tilde{\tau}_*{}^{0.5}\,\tilde{b}}\right\}^{-1} \qquad (15)$$

In **Fig. 11**, the calculated curves ($\tilde{b}$ =1 and 15) of Eq. (14) are compared with the experimental values of β converted by Eq. (15) (using the same data of **Fig. 6**). It can be found that for the values of $\tilde{\tau}_* \geq 0.5$, the β values can be assumed to be nearly constant (average ≈ 0.20), whereas β increases for $\tilde{\tau}_* < 0.5$. The calculated curves of Eq. (14) also show the increasing trend of the β values as decreasing of $\tilde{\tau}_*$ and the minor dependency of β on the extreme values of $\tilde{b}$ similar to the observed values. Therefore, we can assume the model constant β = 0.20 for practical purposes. The identification of β for the sloped-wall abutments is, however, uncertain because of the scarcity of available data, and we should examine this point in the future.

6. CONCLUSIONS

The following points can be concluded from the results discussed in this paper.

(1) For the low value of τ_*/τ_{*c}, the cross-sectional shape of the scour holes is triangular, whereas, trapezoidal shapes of the scour hole are found near the threshold condition of approach flow.

(2) The unit discharges around abutments are found to be more intensified in the scoured bed as compared with that in the flat bed.

(3) From the developed predictive model and the available data ($0.10 \leq b/B \leq 0.30$, $0.15 \leq Fr \leq 0.9$) for vertical-wall abutments, it is proved that b/h is a dominant parameter on d_s/h rather than b/B and Fr.

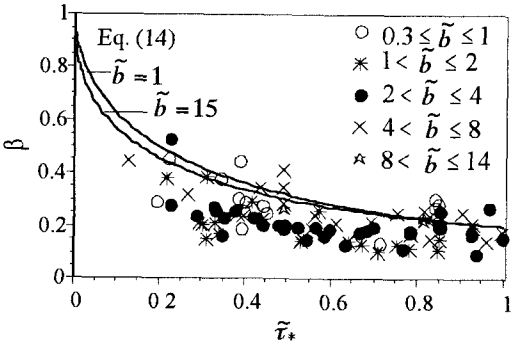

Fig.11 Comparison of calculated curves of Eq. (14) with the observed values of β converted by Eq. (15).

(4) The proposed model will be useful for the prediction of the maximum scour depth around sloped-wall abutments as well as vertical-wall abutments.

(5) The model constant β can be assumed as β = 0.20 for $\tau_*/\tau_{*c} \geq 0.5$ with no dependency on b/h, whereas, for $\tau_*/\tau_{*c} < 0.5$, the β values increases as τ_*/τ_{*c} decreases.

The present model is not available to explain the experimental features of long abutment ($b/h > 25$), where d_s/h takes a constant value (=10) according to Melville's empirical formula[3]. Moreover, the effect of Fr on d_s/h in super-critical flows is uncertain. These are the remaining problems to be solved in the future.

REFERENCES

1) Garde, R.J., Subramanya, K. and Nambudripad, K.D.: Study of scour around spur dikes, J. of the Hydraulic division, ASCE, Vol. 87, Hy6, pp. 23-37, 1961.
2) Tsuchiya, A. and Ishizaki, K.: Scouring around spur-dikes, Proc. of Hydr. Eng., JSCE, Vol. 10, pp. 65~70, 1966 (in Japanese).
3) Melville, B.W.: Local scour at bridge abutments, J. Hydraulic Division, ASCE, 118(4), pp. 615- 631,1992.
4) Laursen, E.M.: An analysis of relief bridge scour, J. Hydraulic. Division, ASCE, Vol. 89(3), pp. 93-118, 1963.
5) Tsubaki, T. and Saito, T.: Bed scouring around spur-dikes, Bulletin of the Faculty of Engineering, Yamaguchi University, Vol. 13, No. 1, pp. 71-80, 1963 (in Japanese).
6) Lim, S.Y.: Equilibrium clear-water scour around an abutment, J. Hydraulic Division, ASCE, 123(3), pp. 237-243, 1997.
7) Michiue, M. and Hinokidani, O.: Calculation of 2-dimensional bed evolution around spur-dike, Proc. of Hydr. Eng., JSCE, Vol. 36, pp. 61~66, 1992 (in Japanese).
8) Shimizu, Y. and Nishimoto, N.: Numerical analyses of bed variation around spur-dike, Res. Rep. of the Civil Eng. Res. Inst. of Hokkaido Develop. Bureau, 1993 (in Japanese).
9) Kawn, R.T.F. and Melville, B.W.: Local scour and flow measurements at bridge abutments, J. of Hydraulic Research, IAHR, 32(5), pp.661~673, 1994.

(Received September 30, 1998)